Singlet-state creation and universal quantum computation in NMR using a genetic algorithm

V. S. Manu* and Anil Kumar†

Centre for Quantum Information and Quantum Computing, Department of Physics and NMR Research Centre, Indian Institute of Science, Bangalore 560012, India

(Received 4 April 2012; published 22 August 2012)

The experimental implementation of a quantum algorithm requires the decomposition of unitary operators. Here we treat unitary-operator decomposition as an optimization problem, and use a genetic algorithm—a global-optimization method inspired by nature's evolutionary process—for operator decomposition. We apply this method to NMR quantum information processing, and find a probabilistic way of performing universal quantum computation using global hard pulses. We also demonstrate the efficient creation of the singlet state (a special type of Bell state) directly from thermal equilibrium, using an optimum sequence of pulses.

DOI: 10.1103/PhysRevA.86.022324 PACS number(s): 03.67.Lx, 03.65.Ud, 82.56.Jn

I. INTRODUCTION

Quantum computation (QC) may possibly be the most remarkable practical application of quantum mechanics [1]. Quantum information processing (QIP) promises, through control of a large quantum system, to perform any quantum algorithm. It holds promise for the efficient solution of some of the difficult problems in computer science, such as integer factorization [2], database search [3], and quantum simulation, which are intractable on any present or future conventional computer [4–7].

The genetic algorithm (GA) is a stochastic global-search method based on the dynamics of natural biological evolution [8]. It was proposed by Holland in 1975 [9]. The GA operates on a population of solutions of a specific problem by encoding the solutions in a simple chromosomelike data structure, and applies recombination operators. At each generation, a new population is created by breeding individuals (selected according to their fitness value) using operations borrowed from natural genetics. This process leads to the evolution of individuals and generates populations that are better suited to their environment. GAs are attractive in engineering design and applications because they are easy to use and are more likely to find the globally optimal solution compared to many other design approaches [10].

Genetic-algorithm optimization has found applications in various fields of physics, such as molecular geometry optimization [11], the prediction of ultrahigh-pressure phases of ice [12], optimization of silicon clusters [13], and determination of best-fit potential parameters for a reactive force field [14].

Long-lasting coherences and high-fidelity controls make nuclear magnetic resonance (NMR) an ideal technique for quantum information processing. They have allowed NMR QIP to experimentally implement several quantum computation algorithms, such as the Deutsch-Jozsa algorithm [15], Grover's database-search algorithm [3], Shor's factorization algorithm [2], preparation of the three-qubit GHZ state [16], dense coding [17], and quantum teleportation [18]. NMR QIP is also well suited for testing basic principles of quantum mechanics [19,20].

The decomposition of a unitary operator as a sequence of experimentally preferable operators is the main task in the experimental implementation of a quantum algorithm. There are several proposals for such decomposition in NMR QIP, such as SMPs (strongly modulated pulses) by Cory *et al.* [21], GRAPE (gradient ascent pulse engineering) by Khaneja *et al.* [22], and the algorithmic approach by Ajoy *et al.* [23]. Here we investigate the use of a genetic algorithm for direct numerical optimization of pulse sequences, and devise a probabilistic method for performing universal quantum computation using hard pulses. GA optimization, being a global-search algorithm, yields unitary decompositions that are more general, and hence can be applied to any spin system with different values of J couplings and chemical shifts [24]. We also investigate quantum state preparation using GA optimization. For performing nonunitary transformations, we have included pulsed-field gradients (PFGs) [25] in GA optimization. We demonstrate hard-pulse unitary decomposition for preparation of the pseudopure state (PPS) and long-lived singlet state (LLSS) (along with the other three Bell states) directly from thermal equilibrium in a two-qubit homonuclear NMR system. Section II of this paper describes the optimization procedure and Sec. III outlines the experimental implementations.

II. GENETIC ALGORITHM FOR NMR PULSE-SEQUENCE GENERATION

In the liquid-state NMR, the system Hamiltonian is composed of the interactions of nuclear spins with the external magnetic field and with each other. By combining that with external radio frequency (rf) pulses (with specific frequency, amplitude, and phase), one can simulate any preferred effective Hamiltonian [26]. Hence the unitary-operator decomposition problem in NMR can be treated as an optimization problem that gives optimal values of pulse parameters and delay durations. Optimality is determined here by a proper fitness function, which depends on the target Hamiltonian or the target state.

We have performed pulse-sequence optimization using GA for quantum logic gates (operator optimization) and quantum state preparation (state-to-state optimization) [21]. State-to-state optimization converges faster than operator optimization

*manuvs@physics.iisc.ernet.in
†anilnmr@physics.iisc.ernet.in

(there can be many operators which can perform the same state-to-state transfer). In the discussion given below, single-qubit rotation (SQR) pulses and two-qubit controlled-NOT (CNOT) gates are operator optimizations, whereas creation of the PPS and Bell states are state-to-state optimizations.

A. Representation scheme

The representation scheme is the method used for encoding the solution of the problem in individuals undergoing genetic evolution. Designing a good genetic representation that is expressive and evolvable is a hard problem in evolutionary computation [8]. Constructing an appropriate representation scheme is the first step in genetic algorithm optimization.

In our representation scheme, we have selected the gene to be a combination of (i) an array of pulses that we apply simultaneously on each channel with arbitrary amplitudes θ and phases ϕ, and (ii) arbitrary delays d between the pulses. It can be easily shown that the repeated application of the above gene forms the most general pulse sequence in NMR. Let an individual representing a valid solution have m genes, and let n be the number of channels or spins. Then the individual can be described as a matrix of size $(n+1)\times 2m$, as shown in Eq. (1):

$$\begin{pmatrix} \theta_{11} & \phi_{11} & . & . & \theta_{m1} & \phi_{m1} \\ \theta_{12} & \phi_{12} & . & . & \theta_{m2} & \phi_{m2} \\ . & . & . & . & . & . \\ . & . & . & . & . & . \\ \theta_{1n} & \phi_{1n} & . & . & \theta_{mn} & \phi_{mn} \\ d_1 & 0 & . & . & d_1 & 0 \end{pmatrix}. \tag{1}$$

This matrix has to be optimized, according to the optimality condition expressed by the fitness function (Sec. II B).

To begin with, we guess the number of genes m as a number that depends on the complexity of the problem to be solved. If the fidelity, i.e., the fitness of the best individual in the population, calculated using the fitness function crosses a cutoff value of, say, >99%, then the optimization program tries to reduce the number of genes by assigning zero values to a few gene parameters. If the fitness function does not cross the cutoff value, then the program will rerun with more numbers of genes. We have carried out the optimization procedure using a population size of 100 individuals evolving for 1000 generations. All of the programs are written in MATLAB in combination with MATLAB's optimization toolbox.

B. Fitness function

A fitness function is a particular type of objective function that describes the optimality of a solution or individual. In operator optimization, GA tries to reach a preferred target unitary operator ($U_{\rm tar}$) from an initial random-guess pulse-sequence operator ($U_{\rm pul}$). We have selected the fitness function $F_{\rm pul}$ to be the projection of $U_{\rm pul}$ onto $U_{\rm tar}$,

$$F_{\rm pul} = {\rm Tr}[(U_{\rm pul})(U_{\rm tar}^{\dagger})]. \tag{2}$$

It is normalized to give the maximum value 1.0 when $U_{\rm pul} = U_{\rm tar}$.

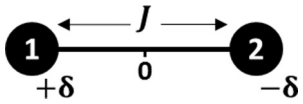

FIG. 1. A two-spin system with chemical shifts $\pm\delta$ and coupling J.

In state-to-state optimization, the optimization program will run over different possibilities of $U_{\rm pul}$ to prepare a preferred target state $\rho_{\rm tar}$ from the initial state $\rho_{\rm in}$. Then we choose the fitness function to be

$$F_{\rm state} = {\rm Tr}\big[(U_{\rm pul})(\rho_{\rm in})\big(U_{\rm pul}^{-1}\big)\big(\rho_{\rm tar}^{\dagger}\big)\big]. \tag{3}$$

In both cases, the optimization has to maximize the fitness function.

III. TWO-QUBIT HOMONUCLEAR CASE

Consider the two-qubit NMR homonuclear system (Fig. 1) with chemical shifts $\pm\delta$ and coupling J. Assuming weak coupling ($\delta \gg J$), the Hamiltonians can be written as [26]

$$H = H_{cs} + H_J = 2\pi\delta(I_{z1} - I_{z2}) + 2\pi J(I_{z1}I_{z2}). \tag{4}$$

For single-qubit rotations in this system, one can use spin selective pulses (low power, long rf pulses), which will excite a small spectral region around the selected spin [27]. On the other hand, by using the natural chemical shift difference between two spins, we show here how to implement SQR with global hard (nonselective) pulses. Later, we extend this method to perform a two-qubit, homonuclear, universal quantum computation using only global hard pulses.

A. Operator optimization

Operator optimization deals with pulse-sequence generation for quantum logic gates. Here we look at two essential unitary operators for universal quantum computation: SQR and the two-qubit CNOT gate.

1. Single-qubit rotations using nonselective pulses

For a two-qubit homonuclear NMR system, we first consider the case $J = 0$,

$$H = H_{cs} = 2\pi\delta(I_{z1} - I_{z2}). \tag{5}$$

Evolution under such a Hamiltonian creates a relative phase among spins, proportional to the chemical shift difference (2δ) and the evolution time. By combining this relative phase with global-rotation hard pulses, single-qubit operations can be performed.

The target operator for SQR is

$$U_{\rm tar} = \exp(-i\theta I_{\phi k}), \tag{6}$$

where $k = 1$ or 2, θ is the flip angle, and ϕ is the phase. The optimized pulse sequence for SQR is shown in Fig. 2. At the start, we selected $m = 3$, i.e., three hard pulses and three delays. The optimized sequence has three hard pulses and a single delay. The flip angle θ of the SQR pulse is determined by the delay and the flip angle of the third pulse, whereas the phase of SQR ϕ and spin selection is determined by phases of all three pulses (Table I). It may be pointed out that single-qubit rotation

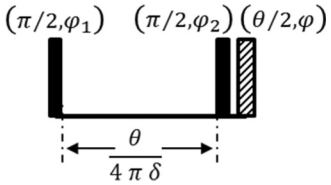

FIG. 2. Pulse sequence for single-qubit rotation. The first two filled pulses are $\pi/2$. The flip angle of the third pulse is $\theta/2$ with phase ϕ. The parentheses above each pulse contain the flip angle (first number) and the phase (second number).

with $\theta = \pi$ is a NOT gate and $\theta = \pi/2$ is a pseudo-Hadamard gate [28].

The experimental verification of the optimized SQR pulse sequence in 5-bromofuroic acid [Fig. 3(a)] (in C_6D_6) is shown in Figs. 3(c) and 3(d). The total length of the pulse sequence for the $\pi/2$ SQR pulse is less than 500 μs, whereas the conventional method (using a selective soft pulse) would need a 2 ms shaped pulse. This substantial (a factor of 4) shortening in time can lead to a significant advantage in quantum circuits.

The above analysis also holds for $J \neq 0$, as long as $\gamma B_1 \gg \delta, J$, except that introduction of the J coupling dephases the final state and results in a fidelity loss. The fidelity of the pulse sequence [fitness function given by Eq. (2)] is studied using a MATLAB simulation (Fig. 4) and is >99.8% for $J/\delta < 0.1$ and $\theta < \pi/2$. ($J/\delta < 0.1$ is the limit for weakly coupled spins and, in this paper, we are dealing with only weakly coupled spins.) For $\pi/2 < \theta < \pi$, the theoretical fidelity is still quite good (>99.5%), as can be seen in Fig. 4.

2. *Controlled-*NOT *gate*

The CNOT gate is an essential component in the construction of a universal quantum computer. Any quantum circuit can be simulated to an arbitrary degree of precision using a combination of CNOT gates and single-qubit rotations [1]. The target unitary operator for C_1NOT_2 is

$$U_{\text{tar}} = \exp\left[-i\left(-\frac{\pi}{4}I + \frac{\pi}{2}I_{x2} + \frac{\pi}{2}I_{z1} - \pi I_{z1}I_{x2}\right)\right]. \quad (7)$$

The optimized pulse sequence for CNOT is shown in Fig. 5(a), obtained using the Hamiltonian of Eq. (4). All four CNOT gates can be obtained by tuning (θ,ϕ), as shown in Table II. The pulse sequence is identical for all four CNOT gates, except for the angles θ and ϕ.

The experimental implementation of various CNOT gates in 5-bromofuroic acid is illustrated in Fig. 5(b). We achieved an average experimental fidelity of 99.9%.

The theoretical fidelity of the CNOT operation [per Eq. (2)] is dependent on the ratio J/δ. The MATLAB simulation of fidelity as a function of J/δ for the CNOT gate pulse sequence is shown in Fig. 5(c). We find that fidelity is >99.99% for $J/\delta = 0.01$ and >99.84% for $J/\delta < 0.1$. This means that even if one needs 10 CNOT gates in a quantum circuit, the fidelity can exceed 99%.

TABLE I. Spin selection and phase ϕ of the SQR is controlled by the phases ϕ_1 and ϕ_2.

Spin to be excited	ϕ_1	ϕ_2
1	$(\phi - \pi/2)$	$(\phi + \pi/2)$
2	$(\phi + \pi/2)$	$(\phi - \pi/2)$

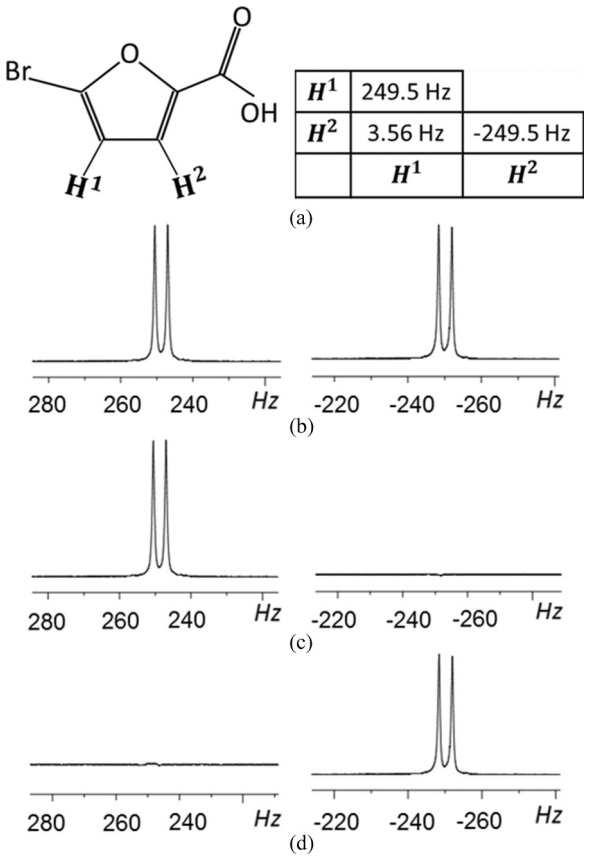

FIG. 3. (a) Chemical structure of 5-bromofuroic acid. Diagonal elements in the table contain the chemical shifts of protons at 500 MHz and the nondiagonal element represents the J coupling (sample dissolved in C_6D_6). (b) Equilibrium spectrum. (c) $(\pi/2)_y$ SQR pulse on spin-1. (d) $(\pi/2)_y$ SQR pulse on spin-2. The average experimental fidelity (calculated using the standard definition [21] that compares spectral intensities with the equilibrium spectrum) for the SQR pulse is 99.9%.

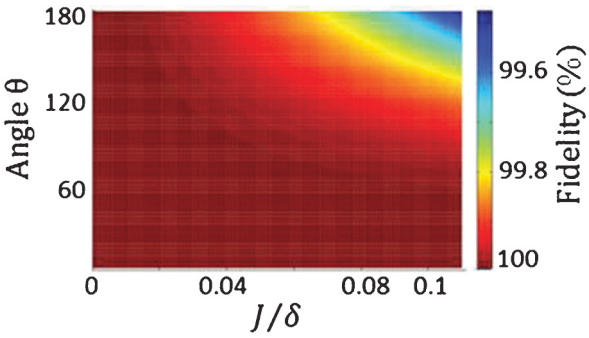

FIG. 4. (Color online) MATLAB simulation study of fidelity variation of SQR with different values of J/δ and θ. As J/δ ratio increases the fidelity is reduced, but is still quite high. For example, for $\theta = 90^\circ$, the fidelity is >99.9% up to $J/\delta = 0.1$ and for $\theta = 180^\circ$, the fidelity is >99.5% for $J/\delta = 0.1$.

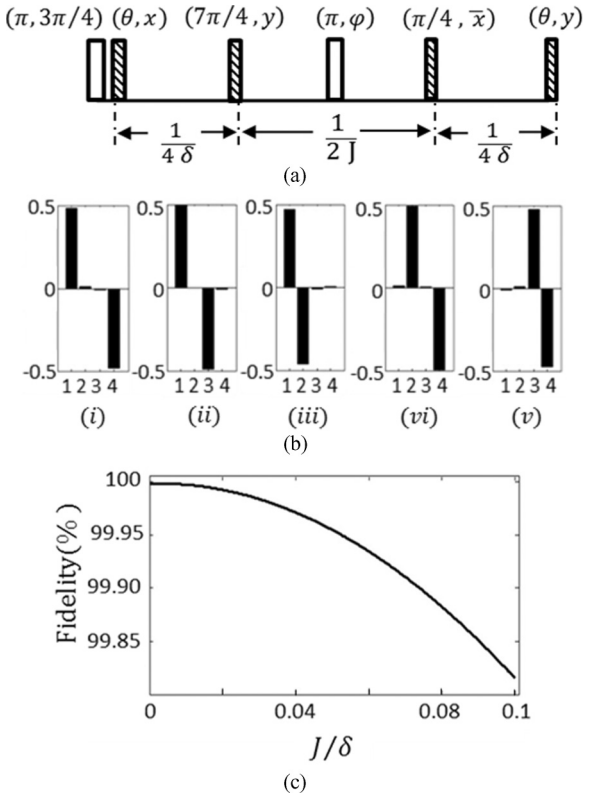

FIG. 5. (a) Pulse sequence for the CNOT gate. The parentheses above each pulse contain the flip angle (first number) and the phase (second number). (b) Diagonal element tomography of (i) the equilibrium state, and the states obtained after applying (ii) C_1NOT_2, (iii) C_2NOT_1, (iv) $\overline{C}_1NOT_2$, and (v) $\overline{C}_2NOT_1$. The labels 1, 2, 3, and 4 represent the states $|00\rangle$, $|01\rangle$, $|10\rangle$, and $|11\rangle$, respectively. An average experimental fidelity of 99.9% is observed (calculated according to Ref. [21] from the diagonal elements of the density matrix). (c) The fidelity F vs J/δ plot for the CNOT gate.

B. State-to-state optimization

State-to-state optimization deals with pulse-sequence generation for quantum state preparation. Here we added gradient pulses to the optimization procedure, which enabled us to perform nonunitary transformations. We show two important quantum state preparations: pseudopure-state creation, and Bell-state creation directly from the mixed thermal equilibrium state using global hard pulses.

TABLE II. (θ,ϕ) values for all four CNOT gates. The notation used is C_iNOT_j, denoting control qubit i and target qubit j. Also $\overline{C_i}$ means that the NOT operation acts on the target when the control qubit is in the $|0\rangle$ state.

Gate	θ	ϕ
C_1NOT_2	$\pi/4$	$\pi/2$
$\overline{C}_1NOT_2$	$\pi/4$	0
C_2NOT_1	$3\pi/4$	0
$\overline{C}_2NOT_1$	$3\pi/4$	$\pi/2$

1. Pseudopure-state creation

Quantum information processing by NMR spectroscopy uses PPS to mimic the evolution and observations on pure states [29]. There are several methods for creating PPS from thermal equilibrium [28–30]. We closely follow the spatial-averaging method (SAM) of Cory *et al*. SAM uses spin-selective pulses, which in homonuclear spin systems become soft, long pulses. Instead, we obtain a novel pulse sequence using only nonselective (hard) pulses for a homonuclear two-qubit system. The optimization problem has the thermal equilibrium state $\Delta\rho_{eq} = I_{z1} + I_{z2}$ as the initial state and $\Delta\rho_{00} = I_{z1} + I_{z2} + 2I_{z1}I_{z2}$ as the target state.

For easier optimization and experimental implementation, we fixed all of the pulses to be $\pi/2$ and optimized only the pulse phases. The resulting sequence consists of six $\pi/2$ pulses and one π pulse for refocusing the chemical shift [Fig. 6(a)]. The phase of the π pulse can be controlled to achieve either the $|00\rangle$ PPS or the $|11\rangle$ PPS. The other PPS's are obtained using a combination sequence of PPS and a SQR π pulse. The experimental results are shown in Fig. 6(b). An average experimental fidelity of 99.5% is obtained for various PPS's.

The theoretical fidelity [using Eq. (3)] of the PPS preparation pulse sequence is also dependent on the ratio J/δ. The

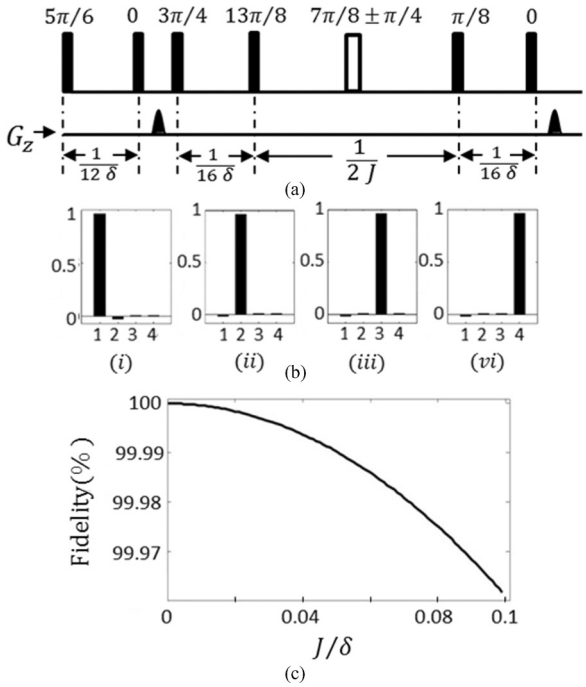

FIG. 6. (a) The pulse sequence for PPS creation. All of the filled pulses are $\pi/2$, and the nonfilled one is π, with the phases written above them. $\pm$ in the phase of the π pulse determines the PPS to be created ($|00\rangle$ or $|11\rangle$). The shaped pulse along G_z represents a PFG pulse, which defocuses all of the transverse magnetization components while retaining the longitudinal magnetization components [25]. (b) Tomography of the diagonal elements after preparing (i) the $|00\rangle$ PPS, (ii) the $|01\rangle$ PPS, (iii) the $|10\rangle$ PPS, and (iv) the $|11\rangle$ PPS. The labels 1, 2, 3, and 4 represent the states $|00\rangle$, $|01\rangle$, $|10\rangle$, and $|11\rangle$, respectively. An average experimental fidelity of 99.5% is observed (calculated according to Ref. [21] from the diagonal elements of the density matrix). (c) The fidelity F vs J/δ plot of the PPS-generation pulse sequence.

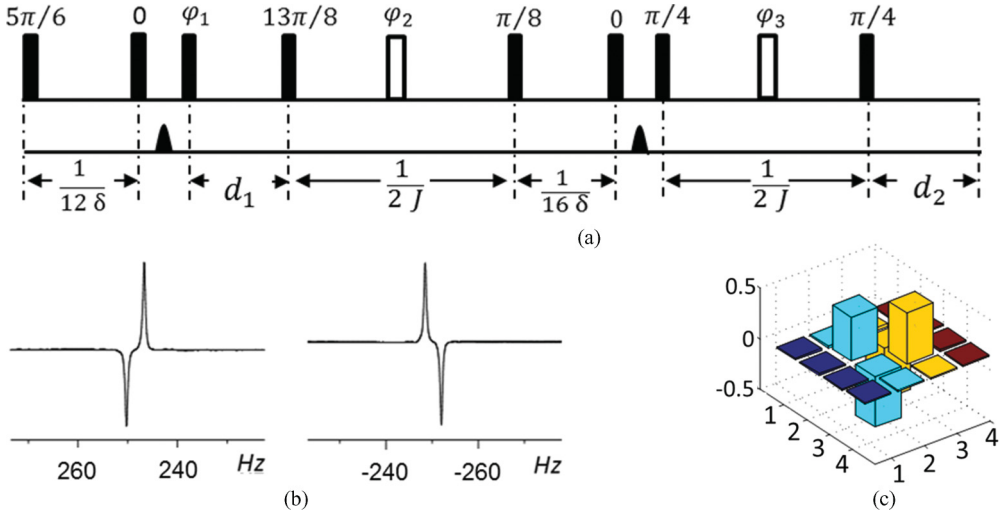

FIG. 7. (Color online) (a) Pulse sequence for creating the Bell states directly from the thermal equilibrium state. All filled pulses are $\pi/2$ and nonfilled pulses are π, with the phases written above them. The shaped pulse along G_z represents a PFG pulse, which defocuses all of the transverse magnetization components, retaining longitudinal magnetization components [25]. The values of ϕ and d are listed in Table III. (b) Observation of the singlet state after applying the operator U of Eq. (9). (c) Density-matrix tomography of the created singlet state. The labels 1, 2, 3, and 4 represent the states $|00\rangle$, $|01\rangle$, $|10\rangle$, and $|11\rangle$, respectively.

MATLAB simulation of this fidelity as a function of J/δ is shown in Fig. 6(c). We observe that fidelity is $>99.9\%$ for $J/\delta < 0.1$.

2. *Creation of Bell states directly from the thermal state*

Bell states are maximally entangled two-qubit states (also known as the Einstein-Podolsky-Rosen states) [31]. They play a crucial role in several applications of quantum information theory. They have been used for teleportation, dense coding, and entanglement swapping [17,18,32]. The creation of Bell states using NMR conventionally requires PPS creation + Hadamard gate + CNOT gate, and hence is demanding [33]. We integrated all of these steps in a single pulse sequence, and optimized that with GA. Again, we kept all pulse amplitudes to be $\pi/2$, and optimized the pulse phases and the delay durations. The optimized pulse sequence [Fig. 7(a)] has 10 nonselective pulses. The final Bell state can be selected by controlling the phase of the pulses and delay durations according to Table III.

The experimental preparation of the Bell state $|\phi^-\rangle = \frac{1}{\sqrt{2}}(|01\rangle - |10\rangle)$, also known as the long-lived singlet state (LLSS), is carried out in 5-bromofuroic acid [34,35]:

$$\rho_{\phi^-} = (0.25I - I_{x1}I_{x2} - I_{y1}I_{y2} - I_{z1}I_{z2}). \tag{8}$$

TABLE III. Values of ϕ and d for Bell-state preparation using the pulse sequence shown in Fig. 7(a).

Bell State	ϕ_1	ϕ_2	ϕ_3	d_1	d_2
$\|\psi^+\rangle = \frac{1}{\sqrt{2}}(\|00\rangle + \|11\rangle)$	$3\pi/4$	$9\pi/8$	$3\pi/4$	$1/16\delta$	0
$\|\psi^-\rangle = \frac{1}{\sqrt{2}}(\|00\rangle - \|11\rangle)$	$3\pi/4$	$9\pi/8$	$\pi/4$	$1/16\delta$	0
$\|\phi^+\rangle = \frac{1}{\sqrt{2}}(\|01\rangle + \|10\rangle)$	0	$5\pi/8$	$3\pi/4$	$9/48\delta$	$9/8\delta$
$\|\phi^-\rangle = \frac{1}{\sqrt{2}}(\|01\rangle - \|10\rangle)$	0	$5\pi/8$	$\pi/4$	$9/48\delta$	$9/8\delta$

The experimental results are shown in Figs. 7(b) and 7(c). Since ρ_{ϕ^-} is not directly observable, we convert the created singlet state into observable single quantum coherence by applying

$$U = (e^{-i(\pi/2)I_{x1}})(e^{-i(\pi/2)I_{x2}})(e^{-i(\pi/4)(I_{z1}-I_{z2})}). \tag{9}$$

An experimental fidelity of more than 99.5% is achieved. The pulse sequence given in Fig. 7(a) is the shortest known pulse sequence for creating a pure singlet state in a two-qubit homonuclear NMR system [36].

The singlet-state lifetime (T_s) was measured by applying the WALTZ-16 spin-lock sequence [37] for a variable time period (0–20 s). We find it to be 11.2 s (Fig. 8), which is longer than $T_1 = 8.7$ and $T_2 = 3.8$ s.

Pulse-sequence generation using GA for larger qubit systems and more complicated operations is in progress. The SQR and CNOT gates implemented using hard pulses (Secs. III A1 and III A2) are valid for larger qubit systems with homonuclear spin pairs (for example, the ^1H-^1H-^{19}F-^{19}F system in 2,3-difluro-6-nitrophenol [27]).

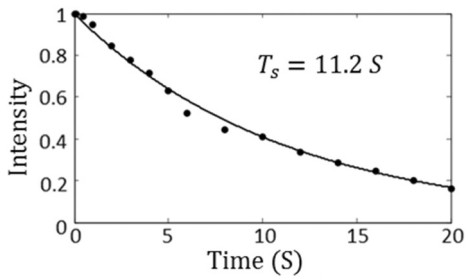

FIG. 8. Antiphase signal decay as a function of interval and fits to a single exponential decay. The initial intensity of singlet state is normalized to one. Observed singlet-state lifetime is $T_s = 11.2$ s. The system has a $T_1 = 8.7$ and $T_2 = 3.8$ s.

IV. CONCLUSION

To summarize, we have used the global-optimization power of a genetic algorithm for (i) efficiently implementing SQR and CNOT gates, and (ii) creating PPS in a homonuclear two-qubit system using only hard pulses. This demonstrates a method for performing universal quantum computation in such systems. We also demonstrated the creation of LLSS and Bell states directly from the thermal equilibrium state, with the shortest known pulse sequence. It should be noted that all of the pulse sequences discussed here are generic, independent of the system and the spectrometer.

ACKNOWLEDGMENTS

We thank Apoorva Patel for discussions and suggestions, and the NMR Research Centre for use of the AV-500 NMR spectrometer. V.S.M. thanks UGC-India for support through a fellowship.

[1] M. A. Nielson and I. L. Chuang, *Quantum Computation and Quantum Information* (Cambridge University Press, Cambridge, UK, 2002).
[2] P. Shor, in *Proceedings of the 35th Annual Symposium on Foundations of Computer Science* (IEEE, Los Alamitos, California, 1994), pp. 124–134.
[3] L. Grover, in *Proceedings of the 28th Annual ACM Symposium on Theory of Computing* (ACM, Philadelphia, 1996), pp. 212–219.
[4] R. Feynman, Int. J. Theor. Phys. **21**, 467 (1982).
[5] A. Aspuru-Guzik, A. Dutoi, P. Love, and M. Head-Gordon, Science **309**, 1704 (2005).
[6] B. Lanyon, J. Whitfield, G. Gillett, M. Goggin, M. Almeida, I. Kassal, J. Biamonte, M. Mohseni, B. Powell, M. Barbieri *et al.*, Nature Chem. **2**, 106 (2010).
[7] J. Du, N. Xu, X. Peng, P. Wang, S. Wu, and D. Lu, Phys. Rev. Lett. **104**, 030502 (2010).
[8] D. Whitley, Stat. Comput. **4**, 65 (1994).
[9] H. John, *Adaptation in Natural and Artificial Systems: An Introductory Analysis with Applications to Biology, Control and Artificial Intelligence* (MIT Press, Cambridge, MA, 1992).
[10] K. Rasheed, H. Hirsh, and A. Gelsey, Artificial Intelligence in Engineering **11**, 295 (1997).
[11] D. M. Deaven and K. M. Ho, Phys. Rev. Lett. **75**, 288 (1995).
[12] M. Ji, K. Umemoto, C. Z. Wang, K. M. Ho, and R. M. Wentzcovitch, Phys. Rev. B **84**, 220105 (2011).
[13] I. Rata, A. Shvartsburg, M. Horoi, T. Frauenheim, K. Siu, and K. Jackson, Phys. Rev. Lett. **85**, 546 (2000).
[14] P. Pahari and S. Chaturvedi, J. Mol. Model. **18**, 1049 (2012).
[15] I. L. Chuang, L. M. K. Vandersypen, X. Zhou, D. W. Leung, and S. Lloyd, Nature (London) **393**, 143 (1998).
[16] R. Laflamme, E. Knill, W. Zurek, P. Catasti, and S. Mariappan, Philos. Trans. A **356**, 1941 (1998).
[17] C. Bennett and S. Wiesner, Phys. Rev. Lett. **69**, 2881 (1992).
[18] C. H. Bennett, G. Brassard, C. Crépeau, R. Jozsa, A. Peres, and W. K. Wootters, Phys. Rev. Lett. **70**, 1895 (1993).
[19] J. R. Samal, A. K. Pati, and A. Kumar, Phys. Rev. Lett. **106**, 080401 (2011).
[20] V. Athalye, S. S. Roy, and T. S. Mahesh, Phys. Rev. Lett. **107**, 130402 (2011).
[21] E. Fortunato, M. Pravia, N. Boulant, G. Teklemariam, T. Havel, and D. Cory, J. Chem. Phys. **116**, 7599 (2002).
[22] N. Khaneja, T. Reiss, C. Kehlet, T. Schulte-Herbrüggen, and S. Glaser, J. Magn. Reson. **172**, 296 (2005).
[23] A. Ajoy, R. K. Rao, A. Kumar, and P. Rungta, Phys. Rev. A **85**, 030303 (2012).
[24] A. Ajoy and A. Kumar, arXiv:0911.5465.
[25] W. Price, Concepts Magn. Reson. **10**, 197 (1998).
[26] R. R. Ernst, G. Bodenhausen, and A. Wokaun, *Principles of Nuclear Magnetic Resonance in One and Two Dimensions* (Oxford University Press, USA, 1990).
[27] T. Mahesh, K. Dorai, A. Kumar *et al.*, J. Magn. Reson. **148**, 95 (2001).
[28] T. S. Mahesh and A. Kumar, Phys. Rev. A **64**, 012307 (2001).
[29] D. Cory, A. Fahmy, and T. Havel, Proc. Natl. Acad. Sci. **94**, 1634 (1997).
[30] N. Gershenfeld and I. Chuang, Science **275**, 350 (1997).
[31] A. Einstein, B. Podolsky, and N. Rosen, Phys. Rev. **47**, 777 (1935).
[32] J.-W. Pan, D. Bouwmeester, H. Weinfurter, and A. Zeilinger, Phys. Rev. Lett. **80**, 3891 (1998).
[33] J. Samal, M. Gupta, P. Panigrahi, and A. Kumar, J. Phys. B **43**, 095508 (2010).
[34] M. Carravetta and M. Levitt, J. Am. Chem. Soc. **126**, 6228 (2004).
[35] G. Pileio, M. Carravetta, and M. Levitt, Proc. Natl. Acad. Sci. **107**, 17135 (2010).
[36] S. S. Roy and T. S. Mahesh, Phys. Rev. A **82**, 052302 (2010).
[37] A. Shaka, J. Keeler, T. Frenkiel, and R. Freeman, J. Magn. Reson. **52**, 338 (1983).